Elastic properties of randomly cross-linked polymers

Sandra J. Barsky and Michael Plischke
Physics Department, Simon Fraser University, Burnaby, British Columbia, Canada V5A 1S6

Béla Joós and Zicong Zhou
Ottawa-Carleton Institute for Physics, University of Ottawa Campus, 150 Louis Pasteur, Ottawa, Ontario, Canada K1N 6N5

(Received 31 May 1996)

We have carried out extensive molecular-dynamics simulations of randomly cross-linked polymers and studied the onset of rigidity as the number of cross-links is increased. We find that for our systems, consisting of chains of length $N=10$, 20, 30, and 50, the shear modulus E vanishes at a concentration of cross-links that is well above the geometric percolation threshold and that it seems to approach zero as $E\sim(n-n_c)^f$, where the exponent f is considerably smaller than either the classical value $f=3$ or the corresponding exponent $t\approx 2.0$ of the conductivity of random resistor networks. [S1063-651X(96)07711-2]

PACS number(s): 82.70.Gg, 78.30.Ly, 64.60.Ak

I. INTRODUCTION

In the process of vulcanization [1] cross-links between molecules on different polymers in a melt convert the system from a fluid to an amorphous solid if the density of cross-links is high enough. The nature of this solid phase with its unusual elastic properties, as well as the transition from the melt, is of considerable interest. In particular, the past few years have seen the development of a replica theory of the vulcanization transition [2–5]. In addition, continuing advances in computational power now make it possible to carry out nontrivial simulations of such complicated systems.

In a previous article [6] two of us have reported on molecular-dynamics simulations that were designed to study the variation of the order parameter and the distribution of localization lengths in the solid phase. These simulations, which involved rather short chains and small system sizes, nevertheless convincingly demonstrated the existence of a universal function $P(\xi)$ that describes the distribution of localization lengths for a wide range of cross-link density. In the present work we extend these simulations to longer polymers and larger systems and focus, in particular, on the shear modulus $E(n)$ as function of the density of cross-links n. The classical theory of rubber elasticity, based on an analogy with percolation on Bethe lattices [7,8], predicts $E\sim(n-n_c)^f$, with $f=3$ as $n\to n_c$, where the critical concentration of cross-links n_c is, in this model, the percolation concentration. Later, de Gennes [9] drew an analogy between the elastic modulus E of a gel and the conductance of a random resistor network and argued that the exponent f that describes the form of E near the percolation transition should be the same as that of the conductance, i.e., $t\approx 2.0$. As pointed out by Feng and Sen in another context [10], this analogy strictly holds only if the interparticle potential (in our case, the cross-linking potential) is ''separable,'' e.g., that of a zero-length spring. In the more general case of an arbitrary spherically symmetric pair potential, the onset of rigidity generically occurs at a larger concentration than does percolation and, moreover, there is no longer a reason to believe that the rigidity exponent is the same as the conductance exponent.

To investigate these and other issues, we have simulated systems consisting of polymers of length $N=$ 10, 20, 30, and 50 monomers with up to 100 chains for the three shorter polymers and 60 chains for the system with $N=$ 50. The polymers were first equilibrated as a melt at a temperature and density equal to those used by Kremer and Grest [11], whose data provided a useful check on our procedures and results. Once an equilibrated melt had been obtained, a fixed number of cross-links was added to the system in the following way. A monomer was selected at random and all other particles within a given distance of this particle were identified. One of these particles was selected at random and connected to the first particle by the same pair potential used to construct the chains, subject to the following exclusions: (i) two particles were not permitted to be linked to each other more than once, (ii) cross-links between nearest neighbors on the same chain were forbidden, and (iii) no particle was permitted to have more than six cross-links. The last of these restrictions in fact was never used: for our cross-link densities, the functionality of all the particles was always less than the maximum. It is worth noting that particles were allowed to cross-link to others on the same chain as long as the distance along the backbone was at least two units. Further details regarding the potentials and other parameters are given in Sec. II.

Once the cross-links had been imposed, the system was again equilibrated before the calculation of the shear modulus and other quantities of interest. There are several methods (discussed in Sec. III) for the calculation of elastic constants and we have tested a number of these for efficiency and accuracy. Most of our results are obtained for a constant energy fixed strain ensemble and thus yield an adiabatic shear modulus. We expect that the behavior near the onset of rigidity will not depend significantly on the choice of ensemble. The bulk of our results are presented in Sec. IV and we conclude this article with a brief discussion in Sec. V.

II. MODEL

We denote the number of polymers in the system by M, the number of monomers on each chain by N, and the cross-

link density, i.e., the number of cross-links per chain, by n. In our model, all particles in the system interact through a purely repulsive truncated Lennard-Jones potential

$$U_{\mathrm{LJ}}(r_{ij})=\begin{cases} 4\epsilon\left[\left(\dfrac{\sigma}{r_{ij}}\right)^{12}-\left(\dfrac{\sigma}{r_{ij}}\right)^{6}+\dfrac{1}{4}\right], & r_{ij}<2^{1/6}\sigma \\ 0\,, & r_{ij}\geqslant 2^{1/6}\sigma, \end{cases} \tag{2.1}$$

which ensures self-avoidance. On a given chain, there is an added attractive potential [12] between nearest neighbors

$$U_{nn}(r_{ij})=\begin{cases} -\dfrac{1}{2}kR_0^2\ln\left[1-\left(\dfrac{r_{ij}}{R_0}\right)^2\right], & r_{ij}<R_0 \\ \infty, & r_{ij}\geqslant R_0, \end{cases} \tag{2.2}$$

with $R_0=1.5\sigma$ and $k=30\epsilon/\sigma^2$. The combination of these two potentials, with the parameters given here, prevents polymers from passing through each other.

Each system was first equilibrated at a density of $\rho\sigma^3=0.85$ and an average temperature $k_BT/\epsilon=1.0$. This was done with a constant energy molecular-dynamics code using a standard velocity Verlet algorithm [13] and periodic boundary conditions. A time step $\delta t=0.005\sqrt{m\sigma^2/\epsilon}$ was used in the integration of the equations of motion and energy was conserved to at least one part in 10^4. Various properties of the melt such as the eigenvalues of the inertia tensor of the chains and the mean square end-to-end distance were monitored and found to be consistent with those in the literature [11].

The cross-links were then imposed on the system according to the following procedure. A particle was selected at random and a list of other particles within a distance of 1.25σ was compiled. One of these particles was then selected at random and tethered to the first particle through the combination of potentials (2.2) and (2.1). Cross-linking between nearest neighbors on the same chain was not allowed nor was more than one link between any pair of particles allowed. This procedure has the virtue that the equilibrium properties of the melt (entanglements and pair correlations) are properly reflected in the statistics of the cross-linking.

In order to further characterize the cross-linked samples, we have calculated a number of geometrical properties of the system. Figure 1 shows the fraction of samples in which the largest cluster percolates in all three directions for $N=10,20$ with $M=100$ and for $N=50$ and $M=60$ plotted as a function of number of cross-links per chain. The data clearly show that the probability of percolation is essentially independent of chain length but strongly depends on the total number of chains. Similar results have been previously reported by Grest and Kremer [14]. While the data are too scanty to perform a proper finite-size analysis, it is clear that percolation occurs for systems of this size for $n\leqslant 0.75$ [15]. Other quantities of interest in connection with rigidity are the number of elastically active segments and the average strand length. An elastically active segment is defined to be any section of a chain between cross-linking points. The strand length is simply the average contour length of such elastically active segments. For all the systems studied, the number of elastically active segments increases more or less linearly with the number of cross-links, as one would expect.

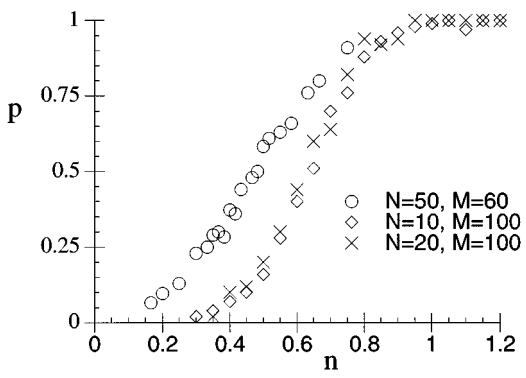

FIG. 1. Plot of the probability p that the system of cross-linked polymers percolates in all three directions as a function of the number of cross-links per polymer n.

The average strand length, on the other hand, does not vary a great deal in the region of interest. Typically, it lies between $N/3$ and $N/4$, which indicates that even in heavily cross-linked systems, most polymers have only two or three linked monomers. It is also worth noting that the average strand length is, in all cases, considerably smaller than the entanglement length, which for these densities was estimated to be $N_e\approx 35$ [11,16].

We note that the cross-linking process introduces a set of quenched random variables, namely the location of the cross-links, into the system. Randomly cross-linked polymers therefore have some of the features of spin glasses and some of the same issues and difficulties with simulations can be expected to arise. For example, it is conceivable that there could be ergodicity breaking or sectioning of phase space. We have partially addressed this in a previous article [6] using an approach of Thirumalai *et al.* [17]. To date we have seen no evidence of sectioning of phase space for a system with a particular realization of cross-links. On the other hand, two samples with the same number of cross-links but with nonidentical realizations clearly access different regions of phase space. It is conceivable that systems with longer chains and longer strand lengths may display ergodicity breaking even for a given cross-linking, but, as mentioned above, we have as yet no evidence for this.

From the perspective of the present calculations, the most important effect of the quenched random variables is that it is necessary to average measured quantities over different realizations of the same number of cross-links. This makes the computations extremely time consuming [18]. For the shorter chains ($N=10,20$) we have typically averaged over 100 different cross-linkings for each value of n, whereas for $N=50$ we have generally obtained our results for 50–60 samples in the vicinity of the transition and for 20 samples in the heavily cross-linked regime. We note also that before a new set of cross-links was imposed on the system, the parent melt was allowed to evolve for several hundred time steps in order to change the configuration of the liquid at least somewhat.

III. CALCULATION OF ELASTIC CONSTANTS

A number of different computational techniques have been used in the past for the calculation of elastic properties

of various condensed systems, most frequently solids. These methods can be broadly divided into fluctuation methods, first introduced by Squire *et al.* [19] and recently discussed in detail by Zhou and Joós [20] and strain methods [1,21]. Most of our results have been obtained by the second of these approaches and we describe it first. In the classical theory of rubber elasticity, the change in free energy of a system undergoing a deformation $L_\alpha \rightarrow \lambda_\alpha L_\alpha$ is assumed to be essentially due to the change in entropy of the elastically active strands. Under the further assumption that the deformation of each strand is affine and that the entropy scales with the square of the strand length (Gaussian chains) one obtains an expression of the form

$$\Delta F = \frac{G}{2}\{\lambda_x^2+\lambda_y^2+\lambda_z^2-3\}, \tag{3.1}$$

where, in this approximation, the modulus G is $G=2N_{\rm el}k_BTb^2\langle r^2\rangle/3$, where $N_{\rm el}$ is the number of strands, b a microscopic length scale, and $\langle r^2\rangle$ the mean-square strand length. Equating this expression to the work done to deform the block, one finds a relation between the modulus G and the stresses applied to the material. For the special case of a pure shear $\lambda_x\lambda_y\lambda_z\equiv 1$ the quantity G is proportional to the shear modulus, which we denote by E and for $\lambda_x\equiv\lambda$, $\lambda_y=\lambda_z=1/\sqrt{\lambda}$ is given by [1]

$$E=\frac{3}{2}G=-\frac{3}{2}\frac{\left[P_{xx}(\lambda)-\frac{1}{3}{\rm tr}\mathbf{P}(\lambda)\right]}{\lambda^2-\lambda^{-1}}, \tag{3.2}$$

where $\mathbf{P}$ is the pressure tensor of the system. For the case of ideal Gaussian chains this expression reduces to $E=N_{\rm el}k_BT/V$. We note that under the less restrictive assumption that the system is an isotropic elastic material, described by elasticity theory with two Lamé coefficients [22], one can show that the shear modulus is given by (3.2) in the limit $\lambda\rightarrow 1$ [see Eq. (3.6)]. As has been shown by Everaers *et al.* [21] for a different system and verified by us for special cases of our cross-linked systems, the right-hand side of (3.2) is essentially independent of λ for values as large as $\lambda=1.8$.

Thus, in this formalism, the calculation of the shear modulus is reduced to the calculation of the diagonal elements of the pressure tensor. This can be straightforwardly done in molecular dynamics (MD) by use of the virial theorem, which yields the expression

$$P_{\alpha\alpha}=\frac{1}{V}\sum_i mv_{i\alpha}^2+\frac{1}{2V}\sum_{i\neq j}F_{ij,\alpha}(r_{i\alpha}-r_{j\alpha}), \tag{3.3}$$

where $F_{ij,\alpha}$ is the α component of the force exerted by particle j on particle i. While each of these components is readily calculated, the final expression (3.2) involves the difference between quantities of the same order of magnitude and the utility of this formula therefore depends on the relaxation time of the components of the pressure tensor. In Fig. 2 we plot the autocorrelation functions

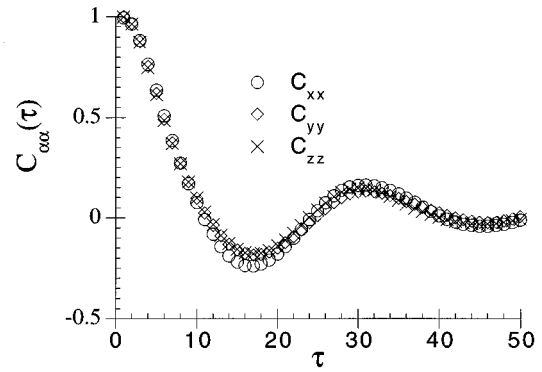

FIG. 2. Plot of the pressure tensor autocorrelation function (3.4) for 60 polymers of length $N=50$ and $N_{\rm cl}=100$ cross-links. The unit of time is the basic MD time step δt.

$$C_{\alpha\alpha}(\tau)=\frac{\langle[P_{\alpha\alpha}(t+\tau)-\overline{P_{\alpha\alpha}}][P_{\alpha\alpha}(t)-\overline{P_{\alpha\alpha}}]\rangle}{\langle[P_{\alpha\alpha}(t)-\overline{P_{\alpha\alpha}}]^2\rangle}, \tag{3.4}$$

where the angular brackets denote averaging over t, for the system of 60 polymers of length 50 with 100 cross-links. The time scale is in units of elementary MD steps. It is clear that the relaxation time of these functions is of the order of $10\delta t$. Thus a typical MD run of $300\,000\delta t$ yields of the order of 30 000 independent samples for E. Separate from the relaxation time in the steady state, there is a characteristic decay time of the initial configuration. This relaxation in the initial regime is shown for the shear modulus for two different samples in Fig. 3, from which we see that the greater part of this transient lasts for roughly $1000\delta t$. The fact that at $t=2000\delta t$ the two shear moduli are essentially the same indicates that there are longer time scales that depend on the number of cross-links that control the decay of the transient. At $t=5000\delta t$ the difference between the two samples is fully apparent. Despite the fact that these characteristic times are quite short, the error bars on the shear modulus are large. Typical values of the components of the pressure tensor for $N=50$ and $M=60$ are $\beta P_{\alpha\alpha}\sigma^3\approx 10.0$, essentially indepen-

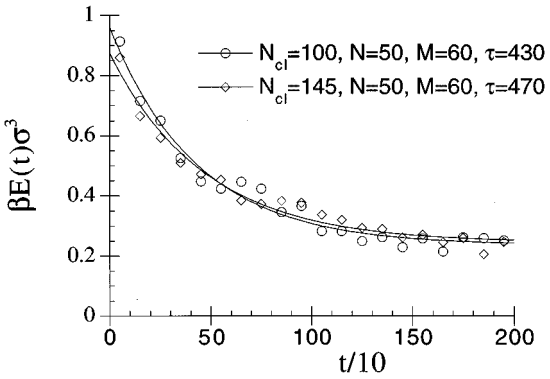

FIG. 3. Time dependence of the dimensionless shear modulus $\beta E\sigma^3$ for early times in a MD run for two numbers of cross-links $N_{\rm cl}=100$ and 145, for the $N=50$, $M=60$ system. The solid curves are fits to the functional form $E(t)=E_\infty+\Delta e^{-t/\tau_0}$ and the data are obtained from an average over 50 different realizations of each cross-linking.

dent of the number of cross-links. On the other hand, $\beta E\sigma^3 \sim 0.1$, so that one needs three-figure accuracy in **P** in order to obtain essentially one significant figure in E. Examining the distribution of values of E over the course of a MD run, one sees that the width of the distribution is roughly 3–4 times the size of the mean.

We note that there are a number of other potential difficulties with the strain method. First, although we expect the liquid to be simply characterized by an isotropic presssure, the imposition of cross-links could produce an internal pressure or some frozen-in stresses that, for small systems, need not be isotropic. One way to reduce the effect of anisotropic frozen-in stresses is to perform the deformation of the system in the three Cartesian directions in turn for each cross-linking. This has the effect of subtracting the contribution from internal stresses from the final result for E for a given cross-linking. It turns out that averaging over a large number of different cross-linkings has the same effect, but the fluctuations in this case are considerably larger. We have also found that the results for a given set of cross-links are quite strongly affected by the initial velocities of the particles, even for our larger systems. This rather surprising effect again disappears when one averages over a large number of initial conditions. Finally, in the derivation of formula (3.2) one assumes that there are no off-diagonal components of the pressure tensor. We have checked this for a number of specific cross-linkings and verified that these terms are essentially zero.

There are two kinds of fluctuation methods: strain-strain fluctuation methods, where the elastic constants are extracted from the fluctuations in the shape of the simulation cell, and the ''equilibrium'' fluctuation method. It is this second one that has been applied to our cross-linked polymer melt. In this method, a formal expression is derived for the elastic constants from the second derivative of the free energy. The elastic constants are directly obtained from the microscopic fluctuations within the system. The method has the advantage that no actual deformations are made, so no symmetry breaking occurs, and all elastic constants can be obtained from a single run. The derivatives are taken with respect to a reference configuration, the one on which virtual deformations are applied for the purpose of calculating the elastic constants. At every step of a computer run, the reference configuration and the volume are the instantaneous ones.

In continuum elasticity theory, the stress-strain relations are [23,24]

$$-P_{\alpha\beta}(\eta) = -P_{\alpha\beta}(0) + c_{\alpha\beta\sigma\tau}\eta_{\alpha\beta}, \tag{3.5}$$

where $c_{\alpha\beta\sigma\tau}$ are elastic stiffness coefficients and $\eta_{\alpha\beta}$ the Lagrangian strain tensor. In our model, $\eta_{11} = -2\eta_{22} = -2\eta_{33} \approx \lambda - 1$ for small deformation and $\eta_{\alpha\beta} = 0$ otherwise. Therefore,

$$\begin{aligned} 2\mu\eta_{11} &\equiv -\left[P_{xx}(\eta) - \frac{1}{3}\mathrm{tr}\mathbf{P}(\eta) - \left(P_{xx}(0) - \frac{1}{3}\mathrm{tr}\mathbf{P}(0) \right) \right] \\ &= \frac{1}{3}\Bigg[2c_{11} - c_{12} - c_{13} - c_{21} - c_{31} \\ &\quad + \frac{1}{2}(c_{22} + c_{23} + c_{32} + c_{33}) \Bigg] \eta_{11}. \end{aligned} \tag{3.6}$$

If the reference state were isotropic, $c_{11} = c_{22} = c_{33}$, $c_{12} = c_{21} = c_{13} = c_{31} = c_{23} = c_{32}$, and $c_{11} - c_{12} = 2c_{44}$ and hence $\mu = c_{44}$ or $\mu = E$, the shear modulus, in the limit $\lambda \to 1$. The frozen-in stresses create a small anisotropy and the above equalities will not be exactly satisfied. For the same reason $P_{xx}(0)$ cannot be assumed to be equal to $\frac{1}{3}\mathrm{tr}\mathbf{P}(0)$.

For a central force system, the expressions for $c_{\alpha\beta\sigma\tau}$ can be written [20]

$$\begin{aligned} c_{\alpha\beta\sigma\tau} = &\frac{1}{V}\left\langle \sum_{i<j} r_\alpha(ij) r_\beta(ij) r_\sigma(ij) r_\tau(ij) \frac{1}{r^2}\left(U'' - \frac{U'}{r} \right) \right\rangle - \frac{1}{k_B T V}\left\langle \delta\left(\sum_{i<j} r_\alpha(ij) r_\beta(ij) \frac{U'}{r} \right) \right. \\ &\left. \times \delta\left(\sum_{i<j} r_\sigma(ij) r_\tau(ij) \frac{U'}{r} \right) \right\rangle - \frac{1}{2V}\left(2\left\langle \sum_{i<j} r_\alpha(ij) r_\beta(ij) \frac{U'}{r} \right\rangle \delta_{\sigma\tau} - \left\langle \sum_{i<j} r_\alpha(ij) r_\sigma(ij) \frac{U'}{r} \right\rangle \delta_{\beta\tau} \right. \\ &\left. - \left\langle \sum_{i<j} r_\alpha(ij) r_\tau(ij) \frac{U'}{r} \right\rangle \delta_{\beta\sigma} - \left\langle \sum_{i<j} r_\beta(ij) r_\tau(ij) \frac{U'}{r} \right\rangle \delta_{\alpha\sigma} - \left\langle \sum_{i<j} r_\beta(ij) r_\sigma(ij) \frac{U'}{r} \right\rangle \delta_{\alpha\tau} \right) + \frac{N k_B T}{V} \delta_{\alpha\beta}\delta_{\sigma\tau}, \end{aligned} \tag{3.7}$$

where $r_\alpha(ij) = r_{i\alpha} - r_{j\alpha}$, $\delta(A) = A - \langle A \rangle$, and U is the total interaction between two particles. The first term in Eq. (3.7) is the Born term, giving the zero-temperature elastic constants, the second is the fluctuation term, the third the stress term, and the last the kinetic term.

A brute-force application of this method in the entropic regime gives $\mu \approx 0$ and $\mu/E \approx 0$, where E is determined by the strain method described above. For instance, in a system of 30 chains of 20 monomers each, this is the case when the number of cross-links is less than 90. It is only when the system becomes more homogeneous and its elasticity is the result of the vibrations of the particles about some equilibrium position that μ/E increases. For the same system as above for 280 cross-links, $\mu/E = 0.836$; for 320 cross-links, $\mu/E = 0.906$; and for 360 cross-links, $\mu/E = 0.974$, close to the expected value of 1. We note that the critical number of cross-links for this system, determined from the point at which the order parameter vanishes, is $N_{\mathrm{cl}} \approx 52$ [6].

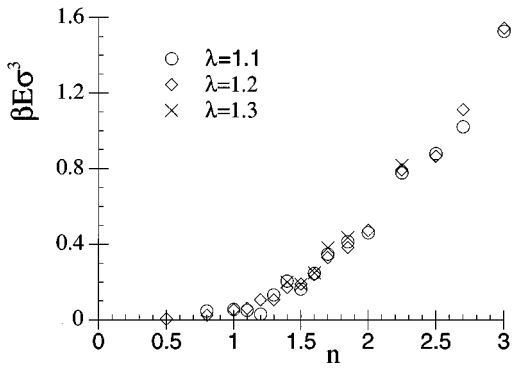

FIG. 4. Plot of the shear modulus determined from the strain method for three different elongations of the computational cell for $N=10$ and $M=100$.

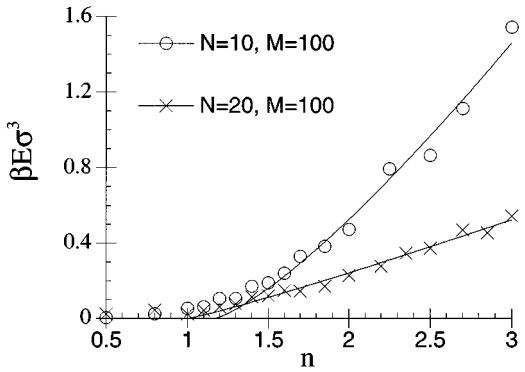

FIG. 5. Plot of the shear modulus for $M=100$ and $N=10,20$ as a function of the number of cross-links per chain. The solid lines are fits of the data to the function $\beta E\sigma^3=b(n-n_c)^f$, with b and f fitting parameters. The critical value of the cross-link density is that determined in [6] from the behavior of the order parameter. The exponents f are 1.11 for $N=10$ and 1.29 for $N=20$.

Why we fail to measure a finite shear modulus even after 10^6 time steps, when the strain method shows a rigid solid, is due to the large fluctuations in the second term of Eq. (3.7), known as the ''fluctuation term.'' This negative term is in fact comparable in size to the sum of the other terms, which are very stable and add up to a positive quantity. This reflects the large amplitude oscillations of the chains at low cross-link densities. The obstacles to the oscillations of the chains generate the rigidity of the melt. Determining how to deal with the fluctuation term holds the key to the application of this method to soft materials of this kind.

IV. RESULTS

As mentioned above, we have primarily used the strain method described in the preceding section to calculate the shear modulus for our cross-linked systems. In Fig. 4 we show the dimensionless shear modulus $\beta E\sigma^3$ as a function of the cross-link density for the system of 100 polymers of length $N=10$ obtained from Eq. (3.2) for $\lambda=1.1$, 1.2, and 1.3. It is clear that there is no trend in the data: all three elongations of the computational cell yield results that are within the statistical errors of one another. However, the fluctuations in the data increase significantly as λ is made smaller. Therefore, we have chosen $\lambda=1.2$ as a compromise between the desire for computational efficiency and the requirement that λ be close to unity. We note that the shear modulus attains a value close to zero near $n\approx1.15$. In our previous study of this system [6], we found that the order parameter of the amorphous phase vanishes at a critical number of cross-links $n_c\approx1.17$, consistent with this behavior. We note that for this finite system, E is nonzero for a range of n below n_c. We believe that this is a finite-size effect of the same kind as seen in Fig. 1, in which the probability that the system percolates increases from 0 to 1 over a range $0.4\leqslant n\leqslant0.8$, whereas for an infinite system this function would be a step function. We expect that ''rigidity percolation'' will likely occur for some realizations of the cross-linkings for $n<n_c$. We also note that the critical cross-link density is a full 60% higher than the percolation probability. While we have no proof that these two numbers will not converge toward each other in the thermodynamic limit, we believe that the difference seen in these finite systems is so large that this is very unlikely.

In Fig. 5 we compare the shear modulus of two systems each with $M=100$ chains and $N=10,20$. We see that the critical cross-link density is quite similar in the two systems, although a study of the order parameter [6] indicates that for $N=20$, $n_c\approx1.01$ as compared to the value of $n_c\approx1.17$ for $N=10$. The most striking feature is the substantial decrease of E with chain length for a given number of cross-links. The classical theory of rubber elasticity [1] predicts $E\sim k_BT/\xi^3$, where ξ is a measure of the mesh size of the system. If we take this mesh size to be the mean strand length, i.e., the mean length of elastically active segments, we obtain $\xi(N=10)/\xi(N=20)\approx0.55$ and therefore a predicted ratio $E(n,N=20)/E(n,N=10)\approx0.17$. This is too small by more than a factor of 2 at even the highest cross-link density. We have not displayed the shear modulus for the system with $N=30$ since it is too small to show much variation on the scale of this figure, but its behavior is qualitatively the same as for the other two chain lengths.

In Fig. 6 we show the dimensionless shear modulus for the largest system ($M=60$ and $N=50$) for which we have reasonably well-converged data. Again, the finite-size effects discussed above are clearly visible. The character of the data changes at $n_c\approx1.4$ from a monotonic decrease to a slower, rather noisy decrease. We again believe that this reflects the

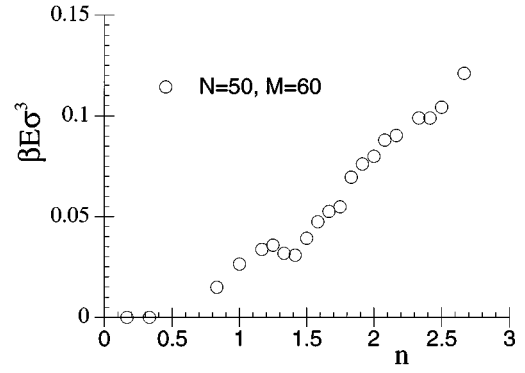

FIG. 6. Shear modulus for $M=60$ and $N=50$ as a function of the density of cross-links.

broad transition in geometric percolation seen in Fig. 1. Unfortunately, we do not have order parameter data for this system and hence no independent determination of the critical cross-link density. However, it is again clear that rigidity percolation occurs at a much higher cross-link density than geometric percolation: for $n=0.6$ none of the samples displayed a finite shear modulus, whereas more than 50% had their largest cluster extend in all three directions through the sample.

One can also attempt to determine an exponent for the variation of the shear modulus near n_c by fitting the data to the form $\beta E\sigma^3=b(n-n_c)^f$. Such fits are shown in Fig. 5 to the data for $N=10,20$. Clearly the quality of the data and the accuracy of n_c do not permit a particularly accurate determination of the exponent f. Both the data of Fig. 5 and those of Fig. 6 yield estimates consistent with $f=1.2\pm0.3$, a value that is much smaller than those previously found for the case of rigidity percolation in three-dimensional lattices with central forces between the particles [25]. However, even in that situation, where significantly larger systems can be studied, there is considerable uncertainty in the value of the exponent f and indeed it is not clear whether or not there is a universal value that depends only on the spatial dimensionality, as do the geometric percolation exponents. What does seem to be clear is that f is different from the conductivity exponent $t\approx2$ of a random resistor network [26] at the geometric percolation threshold, a conclusion also consistent with our result.

If, however, one fits the data of Figs. 5 and 6 to the function $\beta E\sigma^3=b'(n-n^*)^f$, where n^* is the percolation concentration, estimated as described in [15], one obtains larger values for the exponent f. For the two systems with 100 chains, the results are $f\approx1.5$ $(N=20)$, $f\approx1.9$ $(N=10)$, and $f\approx1.3$ for $N=50$ and $M=60$. However, the available data for the order parameter [6] are inconsistent with the picture that these systems become amorphous solids at cross-link densities as small as n^*.

V. DISCUSSION

In this work we have attempted to perform a systematic numerical study of the elastic properties of randomly cross-linked macromolecules near and above the vulcanization transition. While much remains to be done, we believe that we have shown that the percolation theory of rubber elasticity is not valid. As in site- or bond-diluted central force lattices, the transition from a soft inelastic material to material that can withstand shear takes place at a higher concentration of cross-links than is necessary for geometric percolation. However, in contrast to the diluted lattices in which rigidity percolation and geometric percolation occur at the same concentration if there are bond-bending forces, we believe that our result is independent of the nature of the cross-linking potential or of the potential that binds monomers into chains: As long as the strand length, i.e., the typical distance along the chains between cross-linking points, is longer than the persistence length [27] of the chains, the effects of any angular forces are lost.

We have also presented evidence that the exponent f that describes the increase of the shear modulus in the rigid phase is substantially different from the conductivity exponent t of random resistor networks and much less than the classical prediction $f=3$ that follows from a tree approximation. This last result is interesting from the following perspective. de Gennes [29] argued, on the basis of a Ginzburg criterion, that in the limit $N\rightarrow\infty$ the vulcanization transition is described by mean-field exponents. Of course, our chains are very short and our estimates of f in themselves do not refute his theory. However, de Gennes's argument also explicitly assumes that the vulcanization transition occurs at the geometric percolation point, something we believe will not be the case even in the thermodynamic limit. There is clearly a need for further investigation of this issue.

As far as future numerical simulations of such cross-linked systems are concerned, we make the following comments. If the object of the calculation is to obtain more accurate estimates of n_c and of the relevant critical exponents, then it probably pays to increase the number of chains M rather than the chain length N. Figure 1 clearly shows that the geometric percolation transition is sharpened substantially in going from 60 chains to 100 chains and is essentially unaffected by increasing the chain length. While we have only indirect evidence, it seems reasonable to suppose that the same effect will occur at rigidity percolation [28] and therefore larger systems of chains of, e.g., length $N=10$ may provide better data in the critical region. A drawback is that with such short chains one cannot address the aforementioned arguments of de Gennes. A further disadvantage of working with short chains is that the effects of entanglements will certainly be quite minor. As mentioned above, the entanglement length of our systems is of the order of 35 monomers and therefore only the system of polymers with $N=50$ is expected to have a significant number of entanglements. Therefore, in the heavily cross-linked regime it is probably appropriate to study systems as function of N rather than M.

As mentioned in Sec. I, there have been recent developments in the analytic theory of the vulcanization transition [2–5]. The variational approximation of Ref. [3], in which the amorphous state is characterized by a single localization length ξ, predicts $f=2$. The more general theory of [4,5], which allows a distribution of localization lengths, has not yet yielded results for the shear modulus. In addition, the approximations made in these approaches seem to limit the theory primarily to the regime $N\gg1$ and $\langle\xi\rangle\gg1$, where $\langle\xi\rangle$ is the mean localization length of the monomers. With our present computational resources, we are still unable to access this region in parameter space. We note that there have also been some experimental studies of the shear modulus in the context of gelation [30]. These studies have yielded inconsistent results with values of $f\approx2,3$.

Finally, we have noted the discrepancy in estimates of the shear modulus as obtained from strain and fluctuation methods. It remains a challenge to devise an equilibrium fluctuation method that measures accurately the elasticity of a system entropic in nature.

ACKNOWLEDGMENTS

This research was supported by the NSERC of Canada. Two of us (S.J.B. and M.P.) are grateful to Paul Goldbart and G. S. Grest for helpful conversations and correspondence and to C. Homes for computer time.

[1] L.R.G. Treloar, *The Physics of Rubber Elasticity* (Clarendon, Oxford, 1975); Rep. Prog. Phys. **36**, 755 (1973).
[2] P.M. Goldbart and N.D. Goldenfeld, Phys. Rev. Lett. **58**, 2676 (1987); Phys. Rev. A **39**, 1402 (1989); **39**, 1412 (1989); **45**, R5343 (1992).
[3] P.M. Goldbart and A. Zippelius, Phys. Rev. Lett. **71**, 2256 (1993).
[4] H.C. Castillo, P.M. Goldbart, and A. Zippelius, Europhys. Lett. **28**, 519 (1994).
[5] P.M. Goldbart, H.C. Castillo, and A. Zippelius, Adv. Phys. **45**, 393 (1996).
[6] S.J. Barsky and M. Plischke, Phys. Rev. E **53**, 871 (1996). (We note that the notation of this article differs from the present one; there M denotes the number of monomers on a chain and N the total number of particles.) S.J. Barsky, Ph.D. dissertation, Simon Fraser University, 1996 (unpublished).
[7] P. J. Flory, *Principles of Polymer Chemistry* (Cornell University Press, Ithaca, 1953).
[8] P.G. de Gennes, *Scaling Concepts in Polymer Physics* (Cornell University Press, Ithaca, 1979).
[9] P.G. de Gennes, J. Phys. (Paris) Lett. **37**, L1 (1976).
[10] S. Feng and P.N. Sen, Phys. Rev. Lett. **52**, 216 (1984).
[11] K. Kremer and G.S. Grest, J. Chem. Phys. **92**, 5057 (1990).
[12] R.B. Bird, R.C. Armstrong, and O. Hassager, *Dynamics of Polymeric Liquids* (Wiley, New York, 1977), Vol. 1.
[13] M.P. Allen and D.J. Tildesley, *Computer Simulation of Liquids* (Oxford University Press, New York, 1987).
[14] G.S. Grest and K. Kremer, J. Phys. (Paris) **51**, 2829 (1990).
[15] If one estimates the critical cross-link density at which percolation occurs from the expression $n^*=P_\infty(n^*)$, where $P_\infty(n^*)$ is the probability that a cluster spans the system in all directions, one obtains $n^*\approx 0.7$ for $M=100$ and both $N=10,20$ and $n^*\approx 0.5$ for $N=50$ and $M=60$; see e.g., K. Binder and D.W. Heermann, *Monte Carlo Simulation in Statistical Physics* (Springer, Berlin, 1988), Sec. 2.3.
[16] In Ref. [11] the entanglement length N_e was estimated from the equation $g_1(\tau_e)=2\langle R_g^2(N_e)\rangle$. Here $g_1(t)$ is the mean-square displacement of a monomer as a function of time and $R_g(N_e)$ is the radius of gyration of a chain segment consisting of N_e monomers. In the reptation model of polymer dynamics, the time τ_e divides two characteristic regimes $g_1(t)\sim t^{1/2}$ for $t<\tau_e$ and $g_1(t)\sim t^{1/4}$ for $t>\tau_e$.
[17] D. Thirumalai, R.D. Mountain, and T.R. Kirkpatrick, Phys. Rev. A **39**, 3563 (1989).
[18] The calculations reported here consumed several processor years on our cluster of Silicon Graphics workstations.
[19] D.R. Squire, A.C. Holt, and W.G. Hoover, Physica **42**, 388 (1969).
[20] Z. Zhou and B. Joós, Phys. Rev. B **54**, 3841 (1996).
[21] R. Everaers, K. Kremer, and G.S. Grest, Macromol. Symp. **93**, 53 (1995).
[22] L.D. Landau and E.M. Lifshitz, *Theory of Elasticity*, 2nd ed. (Pergamon, New York, 1970).
[23] T. H. K. Barron and M. L. Klein, Proc. Phys. Soc. London **85**, 523 (1965).
[24] J. H. Weiner, *Statistical Mechanics of Elasticity* (Wiley, Toronto, 1983).
[25] C. Moukarzel and P.M. Duxbury, Phys. Rev. Lett. **75**, 4055 (1995); S. Arbabi and M. Sahimi, Phys. Rev. B **47**, 695 (1993).
[26] D.B. Gingold and C.J. Lobb, Phys. Rev. B **42**, 8220 (1990).
[27] The persistence length l_p is defined through the equation $R_{ee}^2=\langle a\rangle^2 l_p^2(N-1)$, where R_{ee}^2 is the square of the end-to-end distance and $\langle a\rangle$ is the average separation between neighboring monomers. In our model $l_p\approx 1.25$.
[28] The size of the critical region for rigidity percolation on generic triangular lattices decreases as $L^{-1/\nu}$ with $\nu\approx 1.2$, where L is the size of the system. See D.J. Jacobs and M.F. Thorpe, Phys. Rev. E **53**, 3682 (1996).
[29] P.G. de Gennes, J. Phys. (Paris) Lett. **38**, L355 (1977).
[30] M. Adam, M. Delsanti, D. Durand, G. Hild, and J.P. Munch, Pure Appl. Chem. **53**, 1489 (1981); M. Adam, M. Delsanti, and D. Durand, Macromolecules **18**, 2285 (1985).